Supplementary Information

High-Throughput Co-Former Screening and Structural Elucidation Using Resonant Acoustic Mixing and 3D Electron Diffraction

Jacob Danks, Daniel N. Rainer, Ahmed S. Hamza, Simon J. Coles, Anthony B. Carter and Joseph E. G. Benson

Experimental procedures

XRPD data was collected in transmission mode on a Bruker D8 Discover using Cu Kα radiation (40 kV, 40 mA), X-ray focusing Göbel mirror, θ - θ goniometer, divergence slit (1.0 mm), Collimator (6 x 1.5 mm) and the SSD160-2 Detector with a 4.5 °2θ to 5.0 °2θ opening without Nickel filter. The software used for data collection was DIFFRAC.COMMANDER version 6.5.0.1 and the data was presented using DIFFRAC.EVA version 4.2.1.11. XRPD diffractograms were acquired under ambient conditions. The data collection range was 3.0 - 40.0 °2θ with a step size of 0.020 °2θ and a collection time of 0.20 seconds per step. Samples were prepared by placing approximately 5 mg powder or slurry into a well of a 96-well plate, suspended with either Mylar or Kapton film.

Raman analysis was performed using the Thermo Scientific DXR3 Raman Microscope equipped with long working distance objective (20 and 50×) and short working objective (10 and 50×) lenses. The instrument can be equipped with a 785 nm laser. The microscope is paired with Olympus (U-TV0.5XC-3) camera which can be viewed using the Thermo Scientific µView software version 9.11. Instrument control along with data acquisition and processing is performed using OMNIC Dispersive for Raman version 9.12. Samples were prepared by distributing a powder over a microscope slide.

DSC analysis was performed on a TA Instruments Q2000 DSC. Approximately 5 mg of material was placed in an aluminium pan and heated at 10 °C/min from 40 °C to the appropriate final temperature. A purge of dry nitrogen at 100 mL/min was maintained over the sample. The instrument control and data acquisition are acquired using Q Advantage software release version 5.5.23. The data was processed and presented using the TA Universal Analysis 2000 software version 4.5A.

3D ED experiments were performed on a Rigaku Synergy-ED electron diffractometer (LaB_6, 200 kV), equipped with a Rigaku HyPix-ED hybrid pixel area array detector. For both samples, the material was gently ground between glass slides and a holey carbon coated copper TEM grid (200 mesh; Agar Scientific, UK) dabbed in the solid. Each grid was then mounted on a Gatan Elsa cryogenic holder and transferred into the instrument using cryo-transfer at 175(5) K.

Grids were surveyed and data collected on a range of particles using CrysAlisPRO (version 1.171.44.47a).[1] All data collections were conducted at 175(5) K in continuous rotation mode using a selected area aperture of about 2 µm diameter in the image plane. Datasets were in each case individually indexed, reduced, and integrated, and subsequently merged and scaled together for each of the two models using CrysAlisPRO (version 1.171.44.127a)[1] and SCALE3 ABSPACK implemented therein. Where necessary, frames were rejected during the processing stage due to holder shadowing and similar effects.

The structures were solved using ShelXT[2] and refined using olex2.refine[3] using the Olex2 GUI (version 1.5-ac7-018) [4] using published scattering factors for electrons[5]. Both models were refined using the kinematical approximation. An extinction correction parameter was refined to account broadly for dynamical effects. All hydrogen atoms could be located in the difference map. They were then placed and refined geometrically constrained, their distances fixed to published X–H distances from neutron diffraction[6], and using IADPs with a riding model with Uiso values fixed to 1.5 of their respective pivot atoms. In the later stages of the refinement, the positions and Uiso values of hydrogen atoms bonded to non-carbon atoms could be refined freely.

RAM screening data

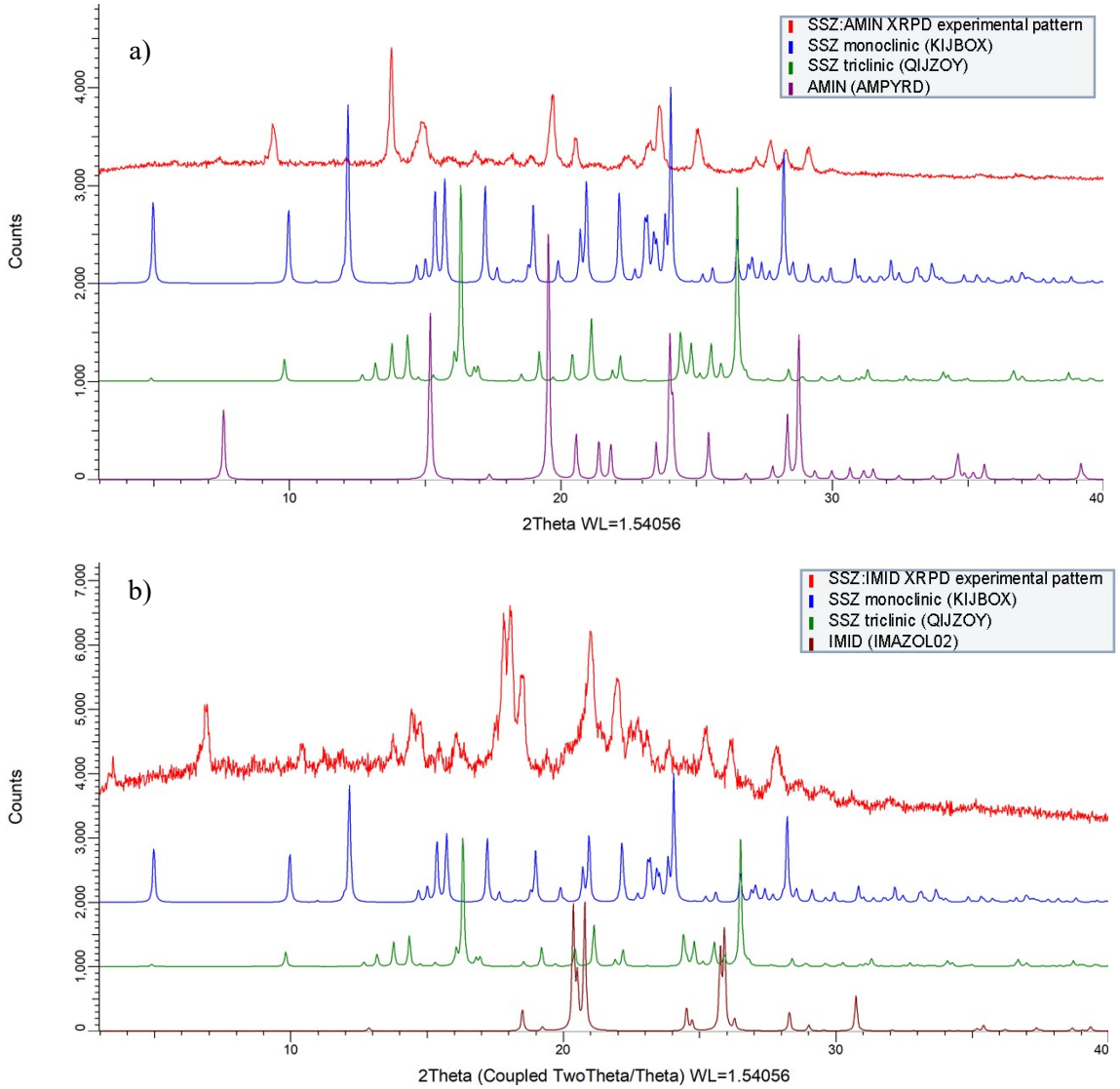

Figure S1: XRPD diffractograms of multicomponent crystals a) SSZ-AMIN; b) SSZ-IMID compared to individual components

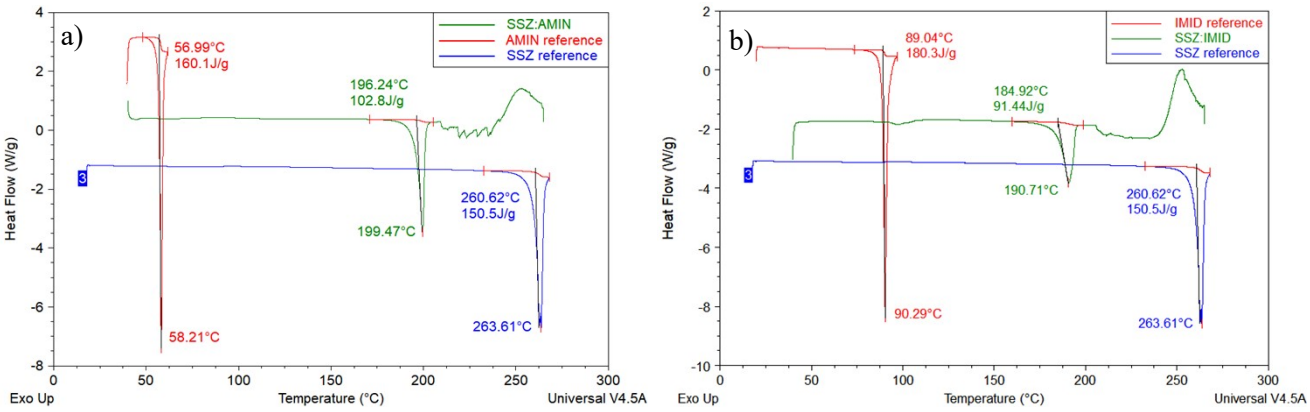

Figure S2: DSC thermograms of multicomponent crystals a) SSZ-AMIN; b) SSZ-IMID compared to individual components

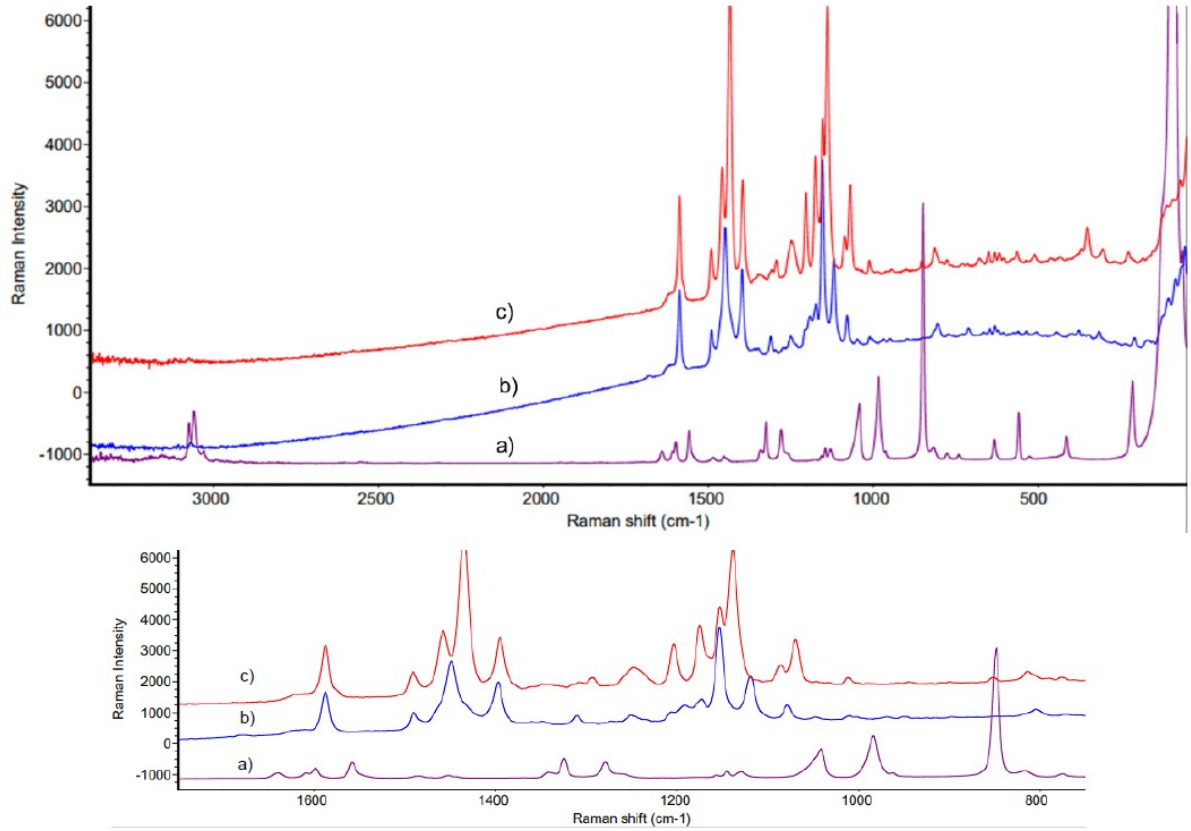

Figure S3: Raman spectrum of a) AMIN reference, b) SSZ reference, c) SSZ-AMIN. The top trace is the full spectrum, the bottom trace is an expansion.

Table S1: Raman peak list for SSZ-AMIN

Region: 3374.51 49.83	
Absolute threshold: 1368.804	
Sensitivity: 81	
Position/ cm^{-1}	**Intensity**
68.41	3417.83
226.58	2263.368
303.55	2311.17
350.65	2660.941
435.45	2179.764
510.79	2222.26
564.02	2273.659
617.17	2244.089
631.13	2249.101
649.64	2267.143
677.93	2159.533
776.60	2134.682
813.95	2329.677
851.92	2128.063
945.11	1983.831
1011.68	2125.329
1069.27	3355.876
1085.98	2516.724
1138.49	6258.806
1152.83	4422.916
1174.78	3820.705
1203.50	3230.491
1248.04	2451.586
1292.97	2127.98
1348.47	1910.864
1394.89	3426.513
1434.64	6848.486
1457.53	3643.038
1490.41	2318.796
1586.97	3187.749

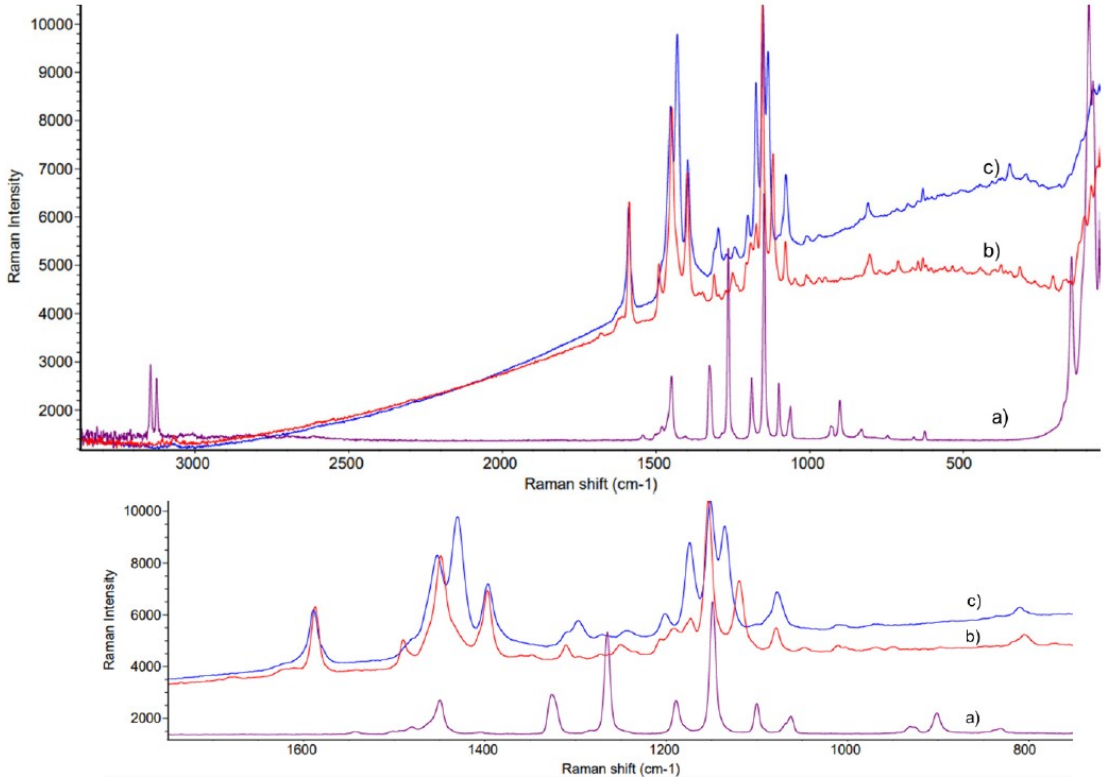

Figure S4: Raman spectrum of a) IMID reference, b) SSZ reference, c) SSZ-IMID. The top trace is the full spectrum, the bottom trace is an expansion.

Table S2: Raman peak list for SSZ-IMID

Region: 3374.51 49.83	
Absolute threshold: 8795.988	
Sensitivity: 75	
Position/ cm^{-1}	**Intensity**
74.86	18932.31
293.67	15069.74
349.09	15525.12
630.9	14418.96
809.44	13749.46
1008.55	12252.79
1077.25	15044.96
1135.15	20646.21
1151.03	22808.82
1173.99	19224.75
1200.79	13200.2
1242.62	11751.28
1270.52	11431.69
1297.14	12623.76
1396.49	15720.67
1430.04	21442.94
1452.46	18152.8

1588.79	13575.5

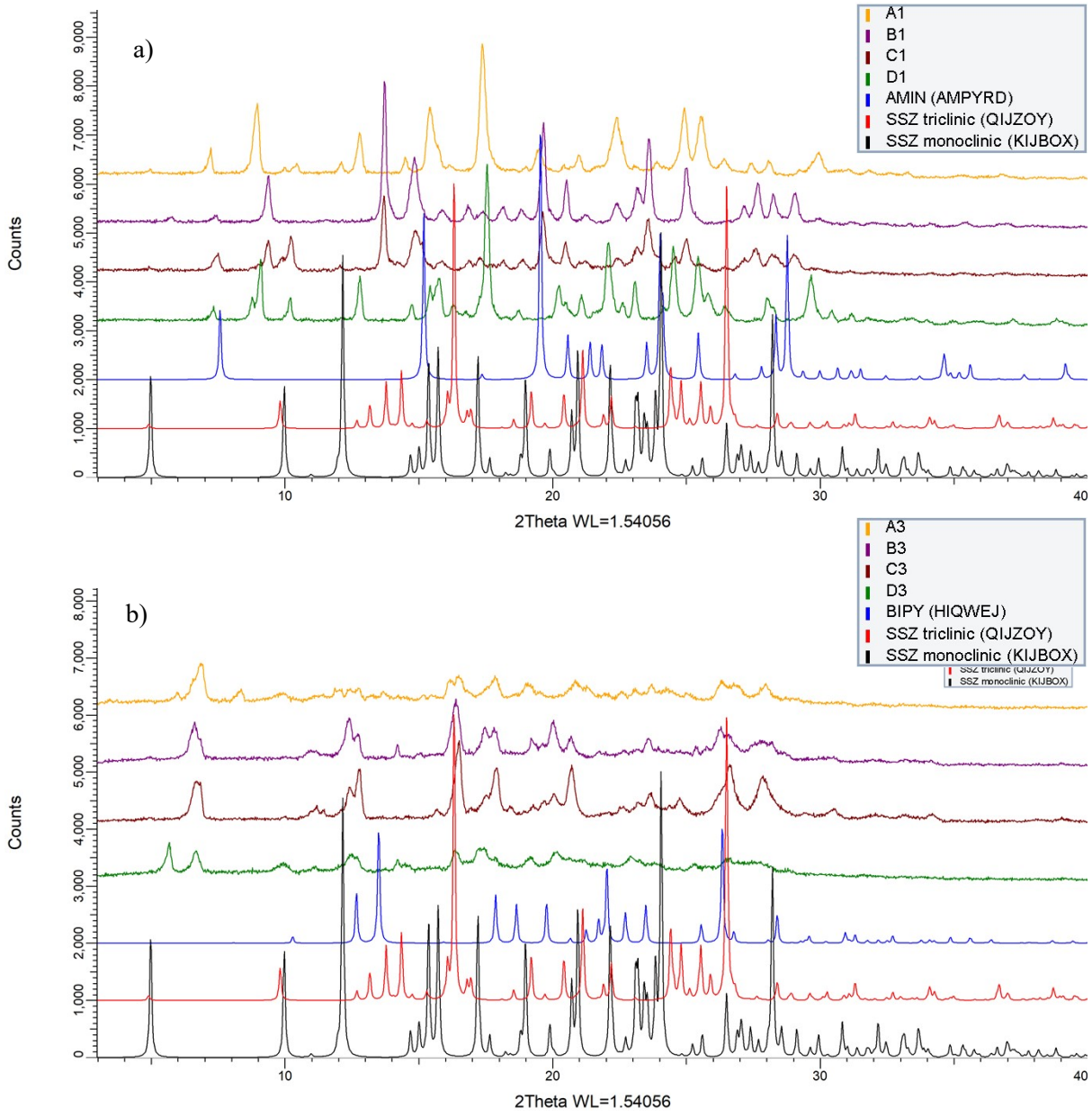

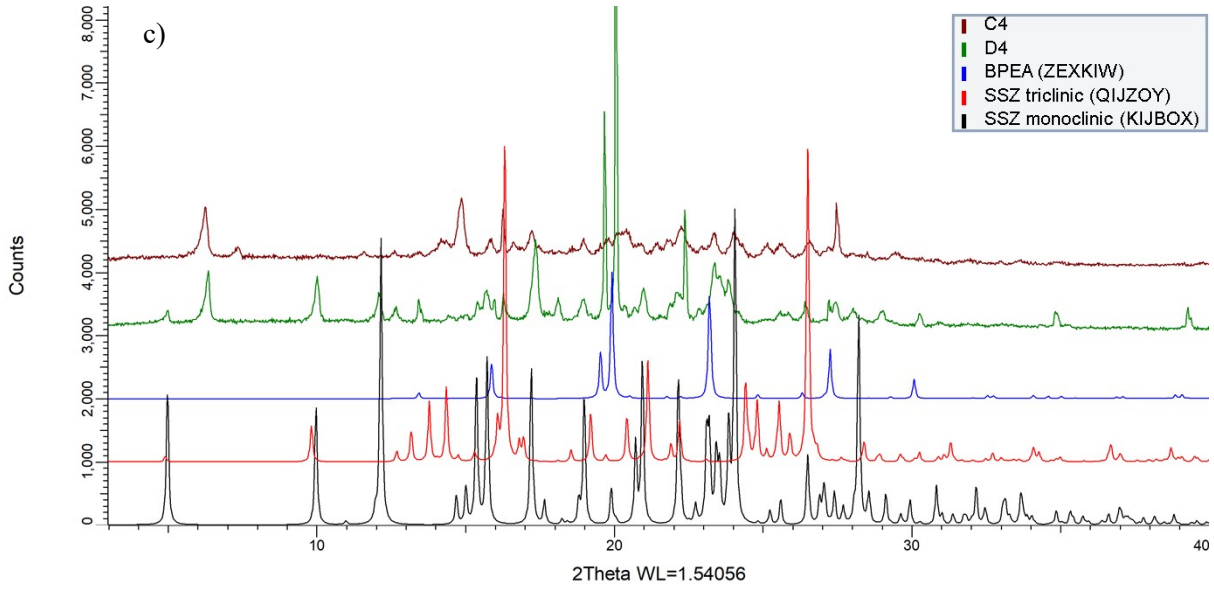
c)
C4
D4
BPEA (ZEXKIW)
SSZ triclinic (QIJZOY)
SSZ monoclinic (KIJBOX)
Counts
0
1,000
2,000
3,000
4,000
5,000
6,000
7,000
8,000
10
20
30
40
2Theta WL=1.54056

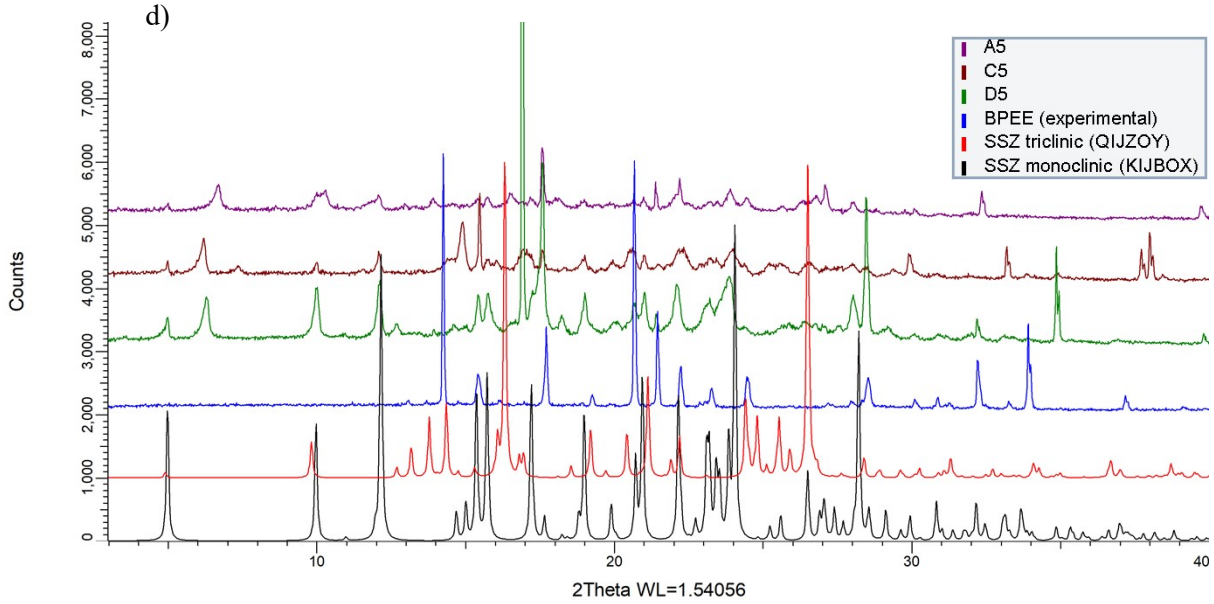
d)
A5
C5
D5
BPEE (experimental)
SSZ triclinic (QIJZOY)
SSZ monoclinic (KIJBOX)
Counts
0
1,000
2,000
3,000
4,000
5,000
6,000
7,000
8,000
10
20
30
40
2Theta WL=1.54056

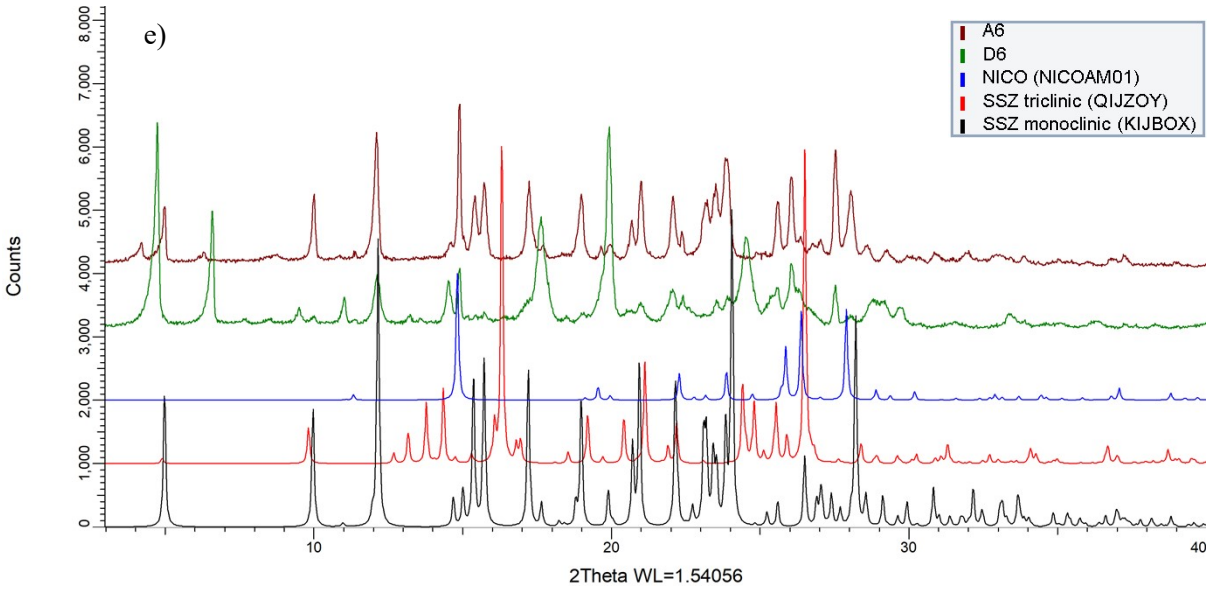
e)
A6
D6
NICO (NICOAM01)
SSZ triclinic (QIJZOY)
SSZ monoclinic (KIJBOX)
Counts
0
1,000
2,000
3,000
4,000
5,000
6,000
7,000
8,000
10
20
30
40
2Theta WL=1.54056

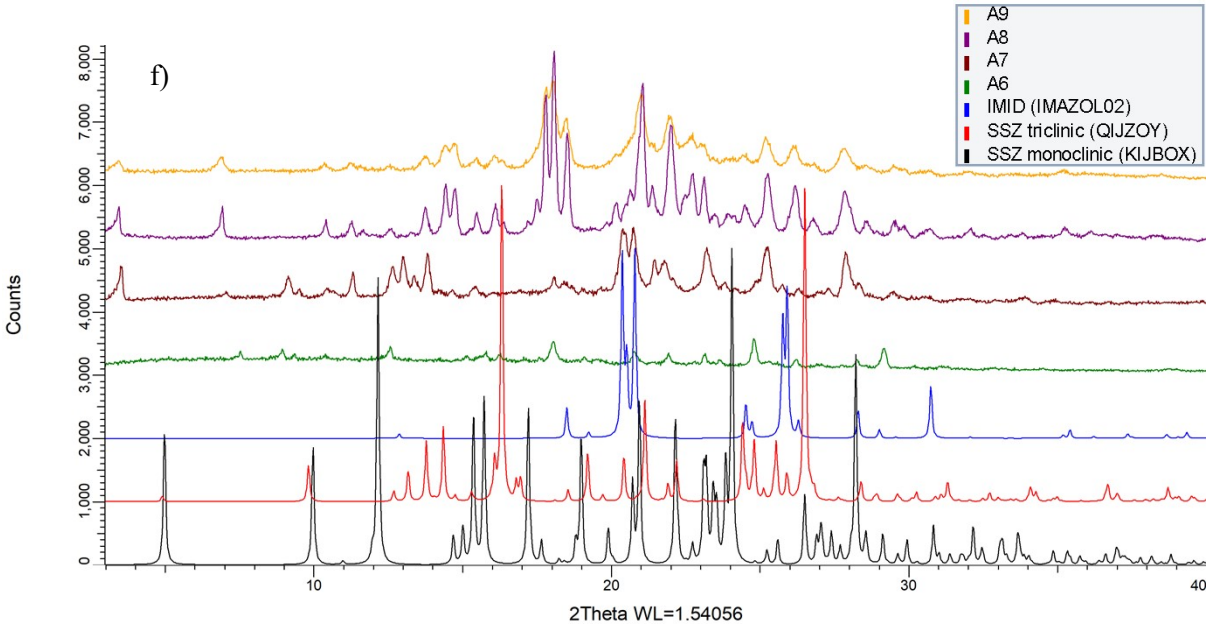
f)
A9
A8
A7
A6
IMID (IMAZOL02)
SSZ triclinic (QIJZOY)
SSZ monoclinic (KIJBOX)
Counts
0
1,000
2,000
3,000
4,000
5,000
6,000
7,000
8,000
10
20
30
40
2Theta WL=1.54056

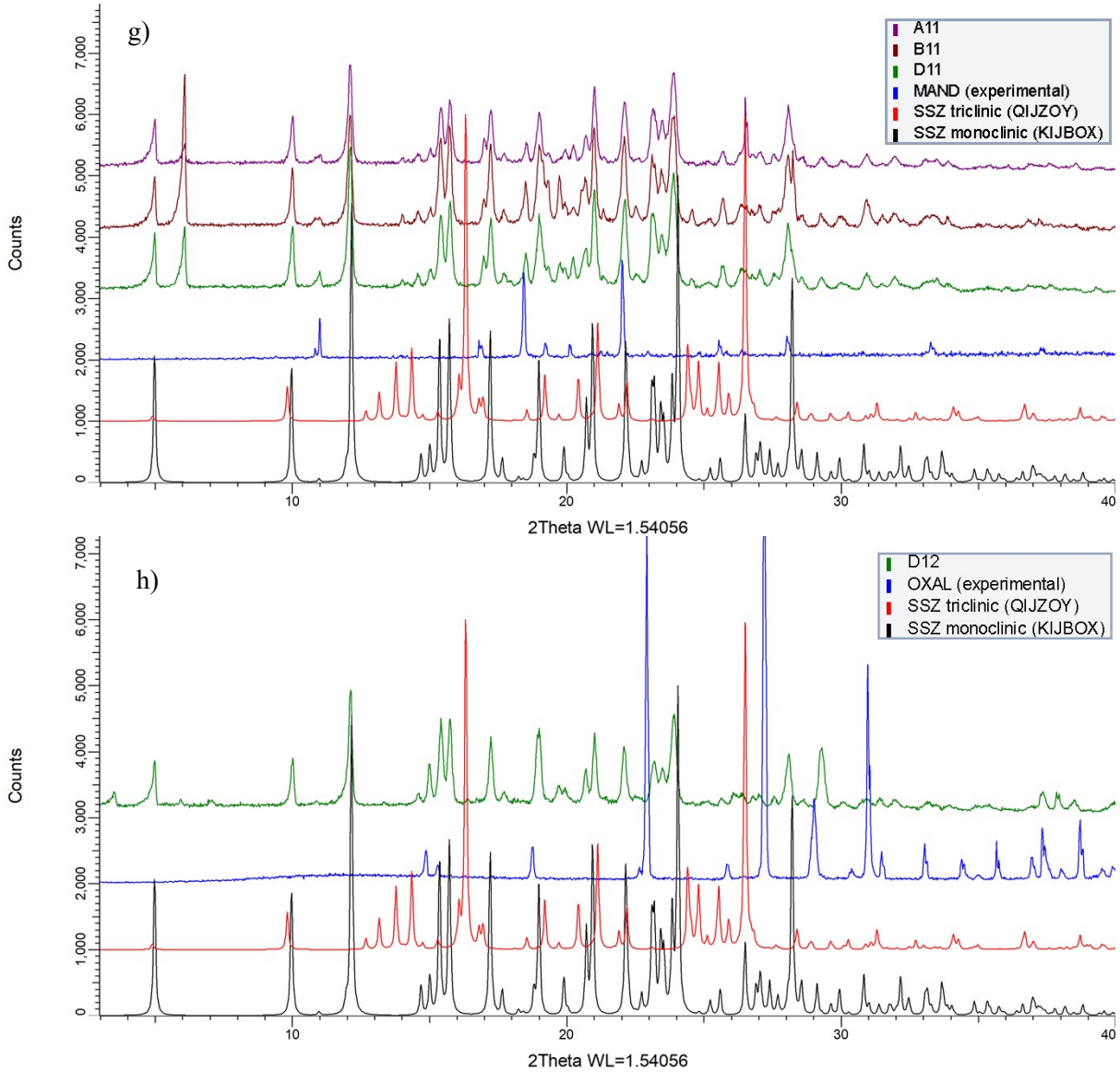

Figure S5: XRPD diffractograms of crystalline hits from RAM screening with: a) AMIN; b) BIPY; c) BPEA; d) BPEE; e) NICO; f) IMID; g) MAND; h) OXAL compared with references

Structural analysis

SSZ-AMIN: In order to further support the location of hydrogen H1 exclusively on N1, the atom was split across N1 and N2 and their occupancies refined. This led to the occupancy factor for H1 refining to approximately unity, providing further evidence for the protonation of the pyridine to pyridinium.

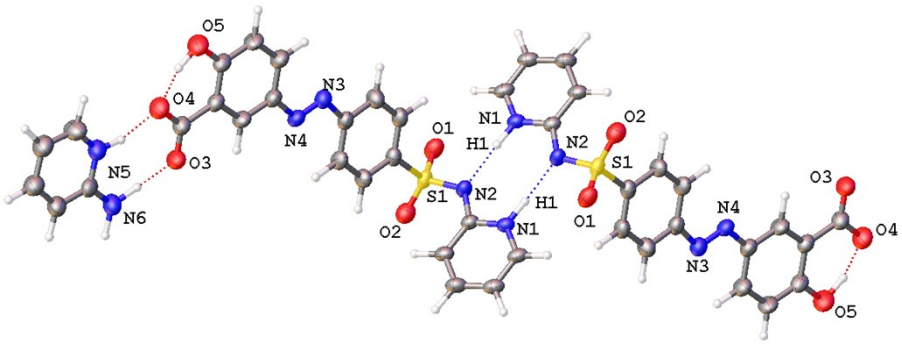

Figure S6: Crystal structure of SSZ-AMIN showing the hydrogen bonding between sulfasalazine and its symmetry-generated neighbour through N1-H1…N2.

SSZ-IMID: Similarly to SSZ-AMIN, the occupancy for the hydrogen atom of pyridine/-ium and sulfonamide/-imide was refined competitively. For the merged dataset, this resulted in an occupancy of 1 for H1, however, an occupancy of about 40% for H5 (pyridinium) and 60% for H6 (sulfonamide). Thus, the crystal structure obtained from the merged dataset was refined against the individual data collections. The results are compiled in Table S3 and show that measured crystals may exhibit either pyridinium or sulfonamide component or indeed the proton being disordered over both sites.

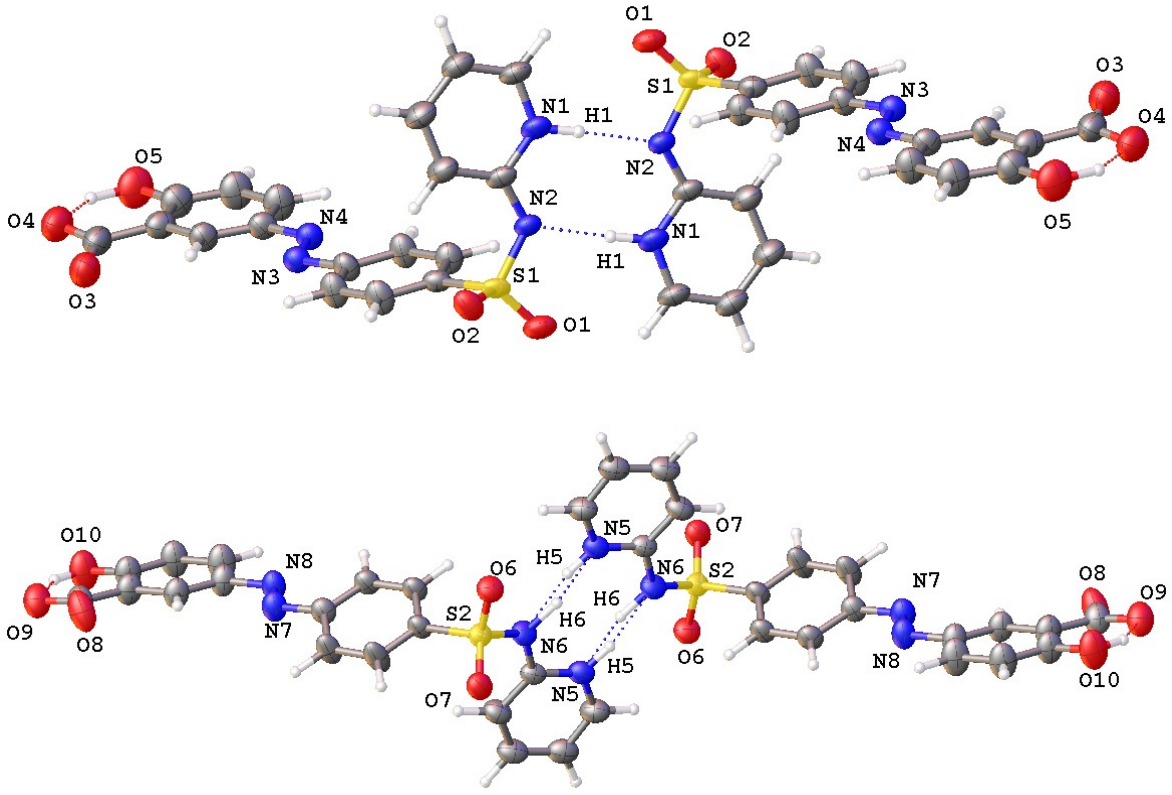

Figure S7: Crystal structure of SSZ-IMID showing the hydrogen bonding between sulfasalazine and its symmetry-generated neighbour through N1-H1…N2 (top) and N5-H5…N6, N6-H6…N5 (bottom).

Complete experimental and refinement information are contained in the deposited CIFs along with structure factors and embedded .RES files. These are deposited in the CSD with CCDC reference codes CCDC 2417286 (SSZ-IMID) and 2417287 (SSZ-AMIN). Tables S4 (SSZ-AMIN) and S7 (SSZ-IMID) report experimental parameters from the used datasets. Figures S8 (SSZ-AMIN) and S9 (SSZ-IMID) show snapshots of the crystals used for the datasets. All raw data can be obtained from https://www.doi.org/10.5281/zenodo.14653435. Final CIF files were checked and edited using CIVET[7].

Table S3: Competitively refined occupancies of hydrogen atoms involved in hydrogen bonding between pyridine/pyridinium (N1-H, N5-H) and sulfonamide/sulfonimide (N2-H, N6-H).

	occupancy "H1" (N1, pyridinium)	occupancy "H5" (N5, pyridinium)
merged dataset	~1	0.42(14)
exp_971	~1	0.1(2)
exp_973	~1	~0
exp_974	~1	~1
exp_978	~1	0.9(2)
exp_980	~1	0.63(12)
exp_981	~1	0.08(17)

Table S4: Crystal data and structure refinement for SSZ-AMIN.

Identification code	SSZ-AMIN
CSD number	2417287
Empirical formula	$C_{23}H_{20}N_6O_5S$
Formula weight	492.516
Temperature/K	175(5)
Crystal system	monoclinic
Space group	*P*2/*n*
a/Å	19.4997(19)
b/Å	6.2871(3)
c/Å	19.695(2)
α/°	90
β/°	106.129(13)
γ/°	90
Volume/Å^3	2319.4(4)
Z	4
ρ_{calc}g/cm^3	1.410
F(000)	386.4
Radiation	electron (λ = 0.0251)
2Θ range for data collection/°	0.1 to 1.8
Index ranges	-24 ≤ h ≤ 24, -7 ≤ k ≤ 7, -24 ≤ l ≤ 24
Reflections collected	32661
Independent reflections	4636 [R_{int} = 0.1838, R_{sigma} = 0.1105]
Refinement theory	kinematical
Data/restraints/parameters	4636/285/335
Goodness-of-fit on F^2	1.053
Final R indexes [I>=2σ (I)]	R_1 = 0.1499, wR_2 = 0.3812
Final R indexes [all data]	R_1 = 0.1908, wR_2 = 0.4054
$\Delta\varphi_{max}$, $\Delta\varphi_{min}$/e Å^{-1}	1.49/-0.91

	Distinct Data Collections				
a/Å	19.5127(12)	19.5501(14)	19.534(2)	19.4644(10)	19.51(2)
b/Å	6.2825(5)	6.3077(4)	6.3073(6)	6.2751(2)	6.305(4)
c/Å	19.7541(13)	19.6676(16)	19.624(2)	19.6875(11)	19.73(4)
α/°	90.163(7)	90.149(7)	89.897(9)	90.073(4)	89.32(11)
β/°	106.118(6)	106.096(8)	105.890(10)	106.027(5)	105.26(14)
γ/°	89.836(6)	89.967(6)	90.103(10)	89.817(4)	90.20(7)
Volume/Å^3	2326.4(3)	2330.3(3)	2325.4(4)	2311.2(2)	2342(5)
h (min, max)	-24, 24	-23, 23	-22, 22	-24, 24	-24, 24
k (min, max)	-7, 7	-7, 7	-7, 7	-7, 7	-7, 7

l (min, max)	-24, 24	-20, 20	-24, 24	-24, 24	-23, 23

Table S5: Selected torsion angles for SSZ-AMIN.

A	B	C	D	Angle/°
N2	S1	C6	C7	-102.0(5)
N2	S1	C6	C11	78.9(5)

Table S6: Hydrogen Bonds for SSZ-AMIN. [1]1-X,2-Y,1-Z.

D	H	A	d(D-H)/Å	d(H-A)/Å	d(D-A)/Å	D-H-A/°
N6	H6a	O3	1.07(4)	1.76(5)	2.833(9)	178(4)
N6	H6b	O3[1]	1.11(4)	1.87(4)	2.829(9)	141(3)
O5	H5a	O4	1.05(4)	1.51(5)	2.519(10)	158(4)
N5	H5b	O4	0.92(5)	1.85(6)	2.738(10)	162(4)

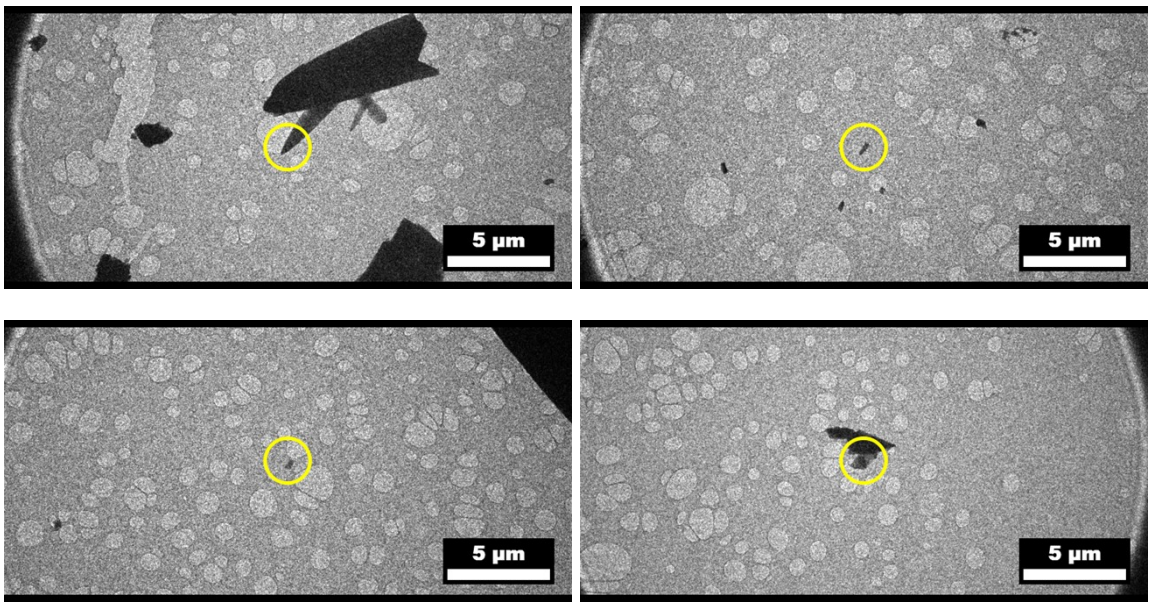

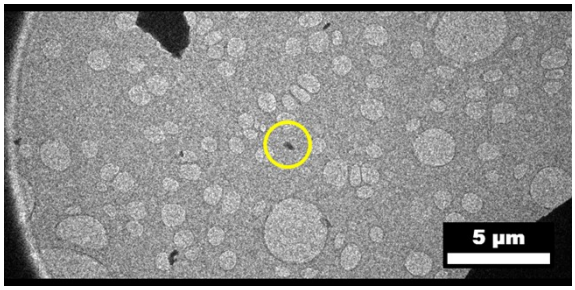

Figure S8: Snapshots of the 5 grains used for SSZ-AMIN. The inset indicates the aperture size of about 2 µm.

Table S7: Crystal data and structure refinement for SSZ-IMID.

Identification code	SSZ-IMID
CSD number	2417286
Empirical formula	$C_{21}H_{18}N_6O_5S$
Formula weight	466.478
Temperature/K	175(5)
Crystal system	triclinic
Space group	*P*-1
a/Å	8.1244(9)
b/Å	10.3705(8)
c/Å	26.277(2)
α/°	80.405(7)
β/°	86.616(9)
γ/°	88.202(7)
Volume/Å^3	2178.7(3)
Z	4
ρ_{calc}g/cm^3	1.422
F(000)	362.1
Radiation	electron (λ = 0.0251)
2Θ range for data collection/°	0.14 to 1.44
Index ranges	$-8 \leq h \leq 8$, $-10 \leq k \leq 10$, $-26 \leq l \leq 26$
Reflections collected	27737
Independent reflections	4505 [R_{int} = 0.2482, R_{sigma} = 0.1578]
Refinement theory	kinematical
Data/restraints/parameters	4505/540/631
Goodness-of-fit on F^2	1.016
Final R indexes [I>=2σ (I)]	R_1 = 0.1325, wR_2 = 0.3723
Final R indexes [all data]	R_1 = 0.1995, wR_2 = 0.4243
$\Delta\varphi_{max}$, $\Delta\varphi_{min}$/e Å^{-1}	0.93/-0.84

	Distinct Data Collections					
a/Å	8.1147(19)	8.1208(16)	8.233(2)	8.1252(14)	8.1352(6)	8.1665(12)
b/Å	10.363(3)	10.376(2)	10.367(3)	10.379(3)	10.3877(10)	10.3537(10)
c/Å	26.358(5)	26.303(7)	26.224(6)	26.427(7)	26.193(2)	26.296(4)
α/°	80.55(3)	80.45(2)	80.16(2)	80.22(3)	80.558(8)	80.335(11)
β/°	87.30(3)	86.817(19)	86.32(2)	86.729(19)	86.607(7)	86.731(12)
γ/°	88.51(2)	88.645(17)	88.25(3)	88.668(19)	87.939(7)	88.130(11)
Volume/Å^3	2183.7(9)	2182.0(8)	2200.4(10)	2192.5(10)	2178.9(3)	2187.7(5)
h (min, max)	-8, 8	-8, 8	-7, 7	-8, 8	-8, 8	-7, 7
k (min, max)	-12, 12	-10, 10	-9, 9	-10, 10	-9, 9	-10, 10
l (min, max)	-31, 32	-26, 26	-26, 26	-25, 25	-22, 22	-24, 23

Table S8: Selected torsion angles for SSZ-IMID.

A	**B**	**C**	**D**	**Angle/°**
N2	S1	C6	C7	51.0(7)
N2	S1	C6	C11	-129.0(7)
N6	S2	C24	C25	42.3(7)
N6	S2	C24	C29	-138.4(8)

Table S9: Hydrogen Bonds for SSZ-IMID. [1]1-X,-Y,-Z; [2]-1+X,+Y,+Z

D	**H**	**A**	**d(D-H)/Å**	**d(H-A)/Å**	**d(D-A)/Å**	**D-H-A/°**
N11	H11a	O8	0.94(10)	1.90(10)	2.696(16)	141(9)
O5	H5a	O4	1.15(7)	1.54(7)	2.571(19)	146(6)
O10	H10	O9	0.96(11)	1.71(11)	2.599(16)	152(10)
N5	H5	N6[1]	1.0(2)	1.8(2)	2.856(15)	179(12)
N6	H6	N5[1]	1.00(19)	1.9(2)	2.856(15)	166(10)
N9	H9	O3	0.90(10)	1.82(10)	2.705(16)	169(9)
N10	H10b	O9[2]	1.16(6)	1.79(6)	2.857(15)	149(5)
N12	H12	O3	1.07(6)	2.03(6)	2.808(19)	128(4)

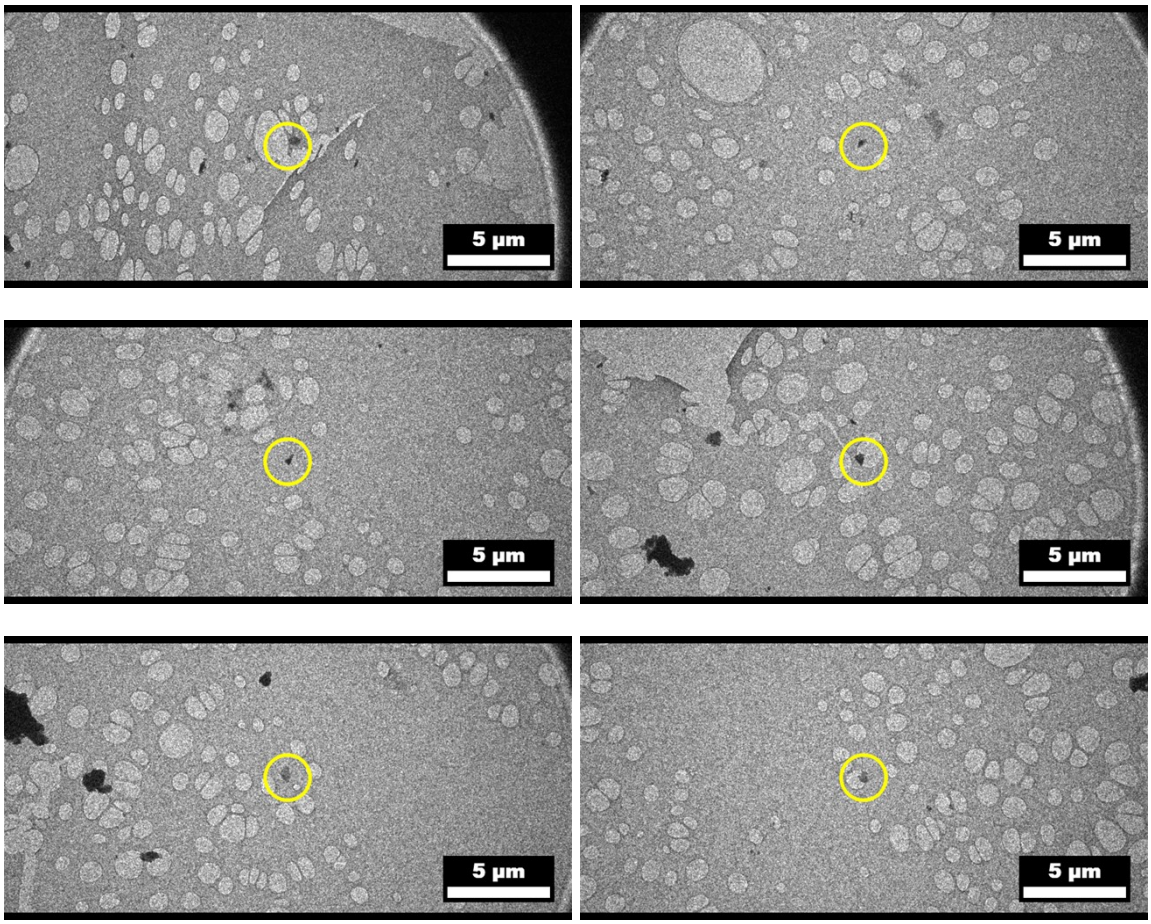

Figure S9: Snapshots of crystals used for SSZ-IMID. The inset indicates the aperture size of about 2 µm.

Rietveld refinement

Constrained Rietveld refinements were performed in Jana2020[8], using the structure models obtained from the 3D ED experiments as models (Figure S10). Atomic positions and atomic displacement parameters were kept fixed for the refinements. A manual background was set and the peak shape approximated using pseudo-Voigt functions. Resulting unit cell parameters and refinement statistics can be found in Tables S10 and S11, respectively.

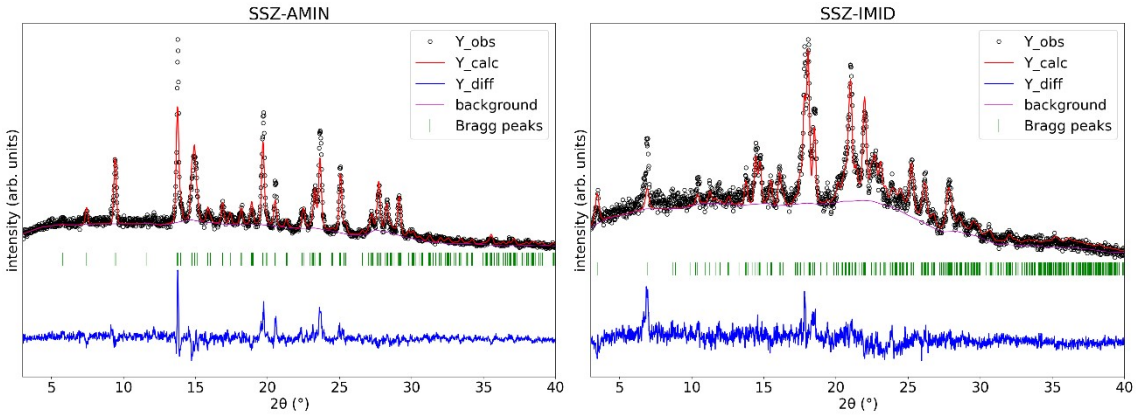

Figure S10: Rietveld refinements plots for SSZ-AMIN and SSZ-IMID. Atom positions and atomic displacement parameters were kept fixed during the refinement.

Table S10: Unit cell parameters obtained from PXRD (Rietveld) and 3D ED refinements.

	SSZ-AMIN		SSZ-IMID	
	PXRD	3D ED	PXRD	3D ED
a [Å]	19.341(8)	19.4997(19)	8.097(4)	8.1244(9)
b [Å]	6.321(2)	6.2871(3)	10.241(7)	10.3705(8)
c [Å]	19.247(5)	19.695(2)	25.81(2)	26.277(2)
α [°]	90	90	80.91(3)	80.405(7)
β [°]	104.38(2)	106.129(13)	86.42(3)	86.616(9)
γ [°]	90	90	87.90(3)	88.202(7)
V [Å^3]	2279.3(14)	2319.4(4)	2108(2)	2178.7(3)

Table S11: Refinement statistics for Rietveld refinements for SSZ-AMIN and SSZ-IMID. Atom positions and atomic displacement parameters were kept fixed during the refinement.

	SSZ-AMIN	SSZ-IMID
Rp	0.093481	0.083662
wRp	0.119074	0.107717

References:

[1] CrysAlisPRO, Rigaku Oxford Diffraction

[2] Sheldrick, G.M., *Acta Cryst. A*, 2015, 71, 3–8.

[3] Bourhis, L. J., Dolomanov, O. V., Gildea, R. J., Howard, J. A. K. & Puschmann, H., *Acta Cryst. A*, 2015, 71, 59–75.

[4] Dolomanov, O. V., Bourhis, L. J., Gildea, R. J., Howard, J. A. K. & Puschmann, H., *J. Appl. Cryst.*, 2009, 42, 339–341.

[5] Saha, A., Nia, S. S. & Rodríguez, J. A., *Chem. Rev.*, 2022, 122, 13883–13914.

[6] Allen, F. H. & Bruno, I. J., *Acta Cryst. B*, 2010, 66, 380–386.

[7] Rainer, D.N. & Hester. J., (2026). danielnrainer/CIVET: v1.2 (v1.2). Zenodo. https://doi.org/10.5281/zenodo.18727982 [8] V. Petříček, L. Palatinus, J. Plášil and M. Dušek, Jana2020 – a new version of the crystallographic computing system Jana, *Zeitschrift für Kristallographie - Crystalline Materials*, 2023, **238**, 271–282. https://doi.org/10.1515/zkri-2023-0005